Preprint
UCRL-JC-148192

A 3D Contact Smoothing Method

M. A. Puso, T. A. Laursen

This article was submitted to
5th World Congress on Computational Mechanics, Vienna, Austria,
July 7-12, 2002

May 2, 2002

This work was performed under the auspices of the United States Department of Energy by the University of California, Lawrence Livermore National Laboratory under contract No. W-7405-Eng-48.

WCCM V
Fifth World Congress on
Computational Mechanics
July 7–12, 2002, Vienna, Austria
Eds.: H.A. Mang, F.G. Rammerstorfer,
J. Eberhardsteiner

A 3D Contact Smoothing Method [1]

Michael A. Puso*

The University of California
Lawrence Livermore National Laboratory
P.O. Box 808 Livermore CA, 94550
e-mail: puso@llnl.gov

Tod A. Laursen

Computational Mechanics Laboratory
Department of Civil and Environmental Engineering
Duke University
Durham N.C. 27708 USA
e–mail: laursen@duke.edu

Key words: contact, finite element, mortar, Bezier, Gregory

Abstract
Smoothing of contact surfaces can be used to eliminate the chatter typically seen with node on facet contact and give a better representation of the actual contact surface. The latter affect is well demonstrated for problems with interference fits. In this work we present two methods for the smoothing of contact surfaces for 3D finite element contact. In the first method, we employ Gregory patches to smooth the faceted surface in a node on facet implementation. In the second method, we employ a Bezier interpolation of the faceted surface in a mortar method implementation of contact. As is well known, node on facet approaches can exhibit locking due to the failure of the Babuska-Brezzi condition and in some instances fail the patch test. The mortar method implementation is stable and provides optimal convergence in the energy of error. In the this work we demonstrate the superiority of the smoothed versus the non-smoothed node on facet implementations. We also show where the node on facet method fails and some results from the smoothed mortar method implementation.

[1] Work performed under the auspices of the U.S. Department of Energy by Lawrence Livermore National Laboratory under Contract W-7405-Eng-48.

1 Introduction

Low order elements such as linear tetrahedrals and tri-liner hexahedrons are typically the element of choice for most finite element analysis, particularly for non-linear analysis. One side effect of low order elements is the non-smooth faceted surface they form. This surface can cause convergence problems for the classical node on facet method [1] due to jumps in surface normals at facet edges. This convergence problem can be alleviated by interpolating the faceted surface with a smooth surface and using the smooth surface to determine contact gap and slip information (Figure 1). A 3D implementation of smoothed node on facet contact was given in [2]. There it was shown that very robust convergence behavior could be achieved with smoothing. An additional benefit to smoothing is the enhanced surface representation it provides, particularly for coarse meshes. The smoothed surface eliminates the "bumping" exhibited by the faceted surfaces when sliding relative to each other and also better resolves interference fits.

On the other hand, the classic method from [1], and the smoothed version [2] are not guaranteed to be Babuska-Brezzi stable. Furthermore, the method will not solve the (flat surface) patch test when elements are warped. In response, approaches using contact elements [3, 4], mortar methods [5, 6, 7, 8] and intermediate contact frames [9] for example, have been developed in an attempt to satisfy the patch test and stability requirements. So far, most of these implementations have been for 2D contact. In this work, we incorporate surface smoothing into a mortar method implementation. The main motivation is to get a better surface representation for such problems as interference fits.

2 Surface Interpolation

2.1 Techniques

The field of Computer-Aided Geometric Design (CAGD) has yielded numerous techniques for 3D surface interpolation [10]. Methods that form composite surfaces from patches seem to be the best suited for finite element implementation since the needed data for the patch interpolation is defined locally. One common interpolation method uses Hermite polynomials to form a C1 interpolation of the surface when a regular mesh is given (Figure 2). Here, a regular mesh is considered one where there is four facets meeting at a vertex everwhere except on surface boundaries.

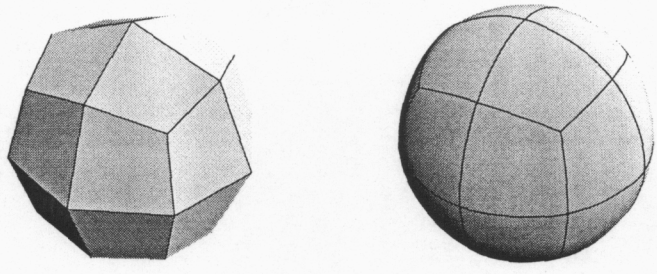

(a) (b)

Figure 1: (a) Finite element mesh of a sphere with surface formed by 24 bilinear facets. (b) Tangent plane continuous surface representation using Gregory patches.

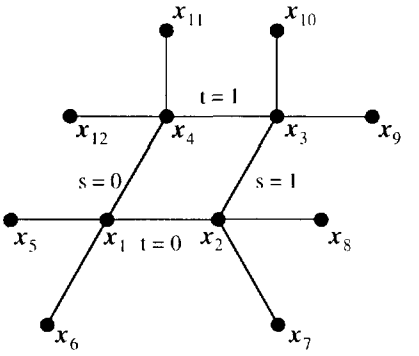

Figure 2: The facet given by coordinates ($\boldsymbol{x}_i, i = 1:4$) with edges from adjacent elements ($\boldsymbol{x}_i, i = 5, 12$) defines a Hermite patch. Isoparametric coordinates s and t are defined as shown.

Following [11], the formula for a Hermite patch is given

$$x_i = \boldsymbol{s} \cdot \boldsymbol{M} \cdot \boldsymbol{G}_i \cdot \boldsymbol{M}^T \cdot \boldsymbol{t}^T \quad (i = 1, 2, 3) \tag{1}$$

$$\text{where} \quad \boldsymbol{s} = \{s^3, s^2, s, 1\}, \quad \boldsymbol{t} = \{t^3, t^2, t, 1\}, \quad \boldsymbol{M} = \begin{bmatrix} 2 & -2 & 1 & 1 \\ -3 & 3 & -2 & -1 \\ 0 & 0 & 1 & 0 \\ 1 & 0 & 0 & 0 \end{bmatrix} \tag{2}$$

$$\text{and} \quad \boldsymbol{G}_i = \begin{bmatrix} x_i(0,0) & x_i(0,1) & x_{i,t}(0,0) & x_{i,t}(0,1) \\ x_i(1,0) & x_i(1,1) & x_{i,t}(1,0) & x_{i,t}(1,1) \\ x_{i,s}(0,0) & x_{i,s}(0,1) & 0 & 0 \\ x_{i,s}(1,0) & x_{i,s}(1,1) & 0 & 0 \end{bmatrix} \tag{3}$$

In our implementation, a zero twist estimation (note the bottom four zeroes) is used in $\boldsymbol{G}_i$ and the parametric derivatives can be defined by differencing adjacent nodes. For example, referring to Figure 2, the derivative at $\boldsymbol{x}(0,0)$ is found

$$\boldsymbol{x}_{,s}(0,0) = 1/2 \ (\boldsymbol{x}_2 - \boldsymbol{x}_5) \tag{4}$$

By rewriting (1), the canonical shape function form for the patch results

$$\boldsymbol{x}(s,t) = \sum_{i=1}^{12} \tilde{N}_A(s,t)\boldsymbol{x}_A \tag{5}$$

where $\tilde{N}_A$ are computed according to (1–3). The problem with this method is that it will only produce C1 continuity everywhere for a regular mesh. In the event of a regular mesh, the method can still be employed but will not provide C1 continuity at vertices.

An alternative patch called the Gregory patch can be used to give G1 (tangent plane) continuity everywhere for an arbitrary mesh. Whereas, the Hermite patch can be viewed as a version of the Bezier patch, the Gregory patch can be viewed as a generalized Bezier patch with the control net shown in Figure 3. The parametric representation for the patch is given

$$\boldsymbol{x}(s,t) = \sum_{i=0}^{3}\sum_{j=0}^{3} B_i^3(s)B_j^3(t)\boldsymbol{x}_{ij}(s,t) \tag{6}$$

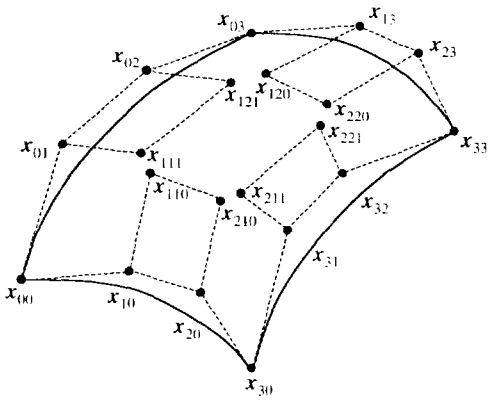

Figure 3: Control net for Gregory patch.

where s and t are the parametric coordinates, B_i^3 are the Bezier functions [10], the interior control points in (6) are written as functions of the surface parameters.

$$\begin{aligned} \boldsymbol{x}_{11}(s,t) &= (s\boldsymbol{x}_{110} + t\boldsymbol{x}_{111})/(s+t) \\ \boldsymbol{x}_{21}(s,t) &= ((1-s)\boldsymbol{x}_{210} + t\boldsymbol{x}_{211})/(1-s+t) \\ \boldsymbol{x}_{12}(s,t) &= (s\boldsymbol{x}_{120} + (1-t)\boldsymbol{x}_{121})/(s+1-t) \\ \boldsymbol{x}_{22}(s,t) &= ((1-s)\boldsymbol{x}_{220} + (1-t)\boldsymbol{x}_{221})/(1-s+1-t) \end{aligned} \tag{7}$$

and the remaining control points are independent of s and t. In [2], the method for determining the appropriate control net (Figure 3) to smoothly interpolate a finite element mesh is developed. In [2], vertex normals are defined at facet vertices by averaging adjacent facet normals. With these vertex normals and coordinates, the formulas from [12] are employed to produce a tangent plane continuous surface. Furthermore, the appropriate friction formulation is developed such that the slip velocity is smooth as nodes transition across element boundaries.

3 Mortar Method

3.1 Mortar Integrals

The mortar method uses integral equations to satisfy the boundary constraint. For mesh tying this amounts to solving

$$\int_\Gamma \boldsymbol{\mu} \cdot (\boldsymbol{u}^1 - \boldsymbol{u}^2)\, d\Gamma = 0 \tag{8}$$

where $\boldsymbol{u}^i$ $i = 1,2$ are the displacements on the non-mortar and mortar side respectively and $\boldsymbol{\mu}$ is the Lagrange multiplier interpolation field. In the proposed smoothed mortar method implementation (Figure 4), a smoothed surface (Γ^2) is tied to the faceted finite element surface (Γ^1) using (8). The smooth surface adopts the identical mesh as side 1 but uses the interpolation given by (5). The following discretizations for $\boldsymbol{\mu}$, $\boldsymbol{u}_1$ and $\boldsymbol{u}_2$

$$\boldsymbol{\mu} = \sum_{A=1}^{n_l} \hat{N}_A \boldsymbol{\mu}_A, \quad \boldsymbol{u}^1 = \sum_{B=1}^{n^1} N_B^1 \boldsymbol{u}_B^1, \quad \boldsymbol{u}^2 = \sum_{B=1}^{n^1} \tilde{N}_B^2 \boldsymbol{u}_B^2 \tag{9}$$

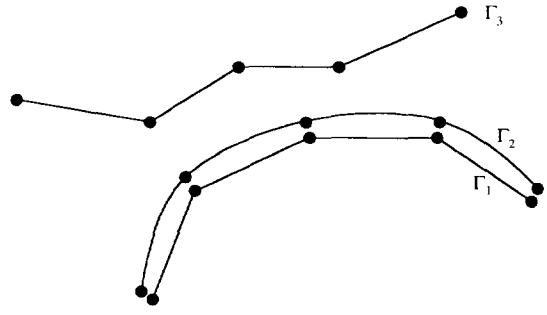

Figure 4: Smooth surface Γ_2 tied to mesh surface Γ_1. Contacting surface shown as Γ_3.

are used in (8) where N_A^1 are the standard bilinear shape functions defined for the n^1 nodes on the non-mortar surface and $\tilde{N}_A^2$ are the shape functions from (5) (re-numbered). A variety of forms for $\hat{N}_A$ exists for the multiplier interpolation but the most convenient for this implementation is the dual formulation given in [13]. As shown in [14], the displacements $\boldsymbol{u}_A^1$ can effectively be eliminated from the system and replaced by a weighted sum of the displacements $\boldsymbol{u}_A^2$. Now a mortar implementation of unilateral contact is applied between surfaces Γ^2 and Γ^3. A number of mortar contact methods have been proposed e.g. [5, 6, 7, 8] although most were not developed for large deformations. One possible large deformation implementation uses the constraint metric

$$\boldsymbol{v}_A = \int_\Gamma \hat{N}_A(\boldsymbol{x}^2 - \boldsymbol{x}^3)\, d\Gamma = 0 \tag{10}$$

For normal contact (i.e. no friction), a "normal" is need to determine the amount of penetration One definition would be to average the normal over the facets which intersect the support for shape function A to produce a mean normal $\bar{\boldsymbol{\nu}}_A$. The contact gap, pressure and unilateral constraint are then defined (no sum over A):

$$g_A = \boldsymbol{v}_A \cdot \bar{\boldsymbol{\nu}}_A, \quad \boldsymbol{\mu}_A = p_A \bar{\boldsymbol{\nu}}_A, \quad p_A \cdot g_A = 0, \quad p_A \geq 0, \quad g_A \geq 0. \tag{11}$$

4 Examples

4.1 Example 1: rotating spheres with friction using node on facet algorithm

In this example, taken from [2], smooth and non-smoothed node on facet contact is compared. An interference fit of concentric spheres is used to demonstrate the superior accuracy of surface smoothing. A spherical shell ($R_i = 1.0$, $R_o = 1.1$) is composed of a thermal material [2] with $E = 5 \times 10^{10}$, $\nu = 0$, $\alpha = 1 \times 10^{-5}$ and surrounded by two rigid spherical shells (Figure 5). The central flexible shell is connected (merged) to the outer rigid shell and separated by a contact surface from the inner rigid shell. Augmented Lagrange contact with a Coulomb friction coefficient of $\mu = 0.1$ was employed. The loading sequence is as follows:

1. In the first time step, the central spherical shell is heated 1000 temperature units thus applying a thermal strain of 0.01

[2] $\alpha \equiv$ thermal expansion coefficient

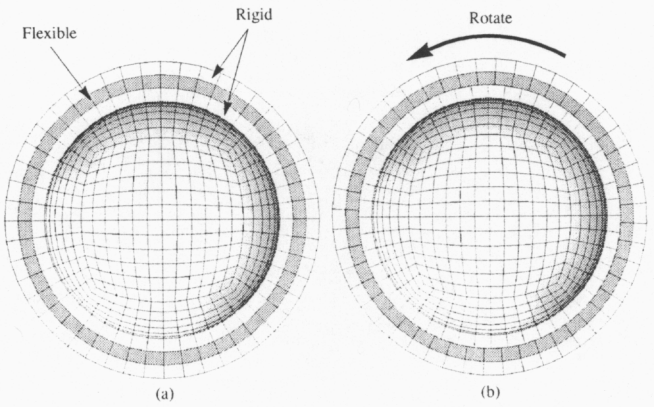

Figure 5: Concentric spheres (864 elements) demonstrated in example 1.

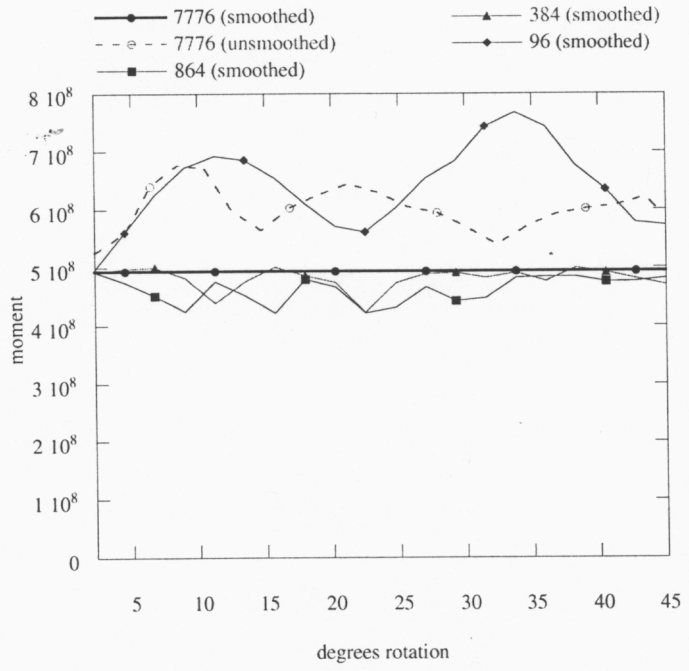

Figure 6: Moment versus rotation from rotating concentric spheres.

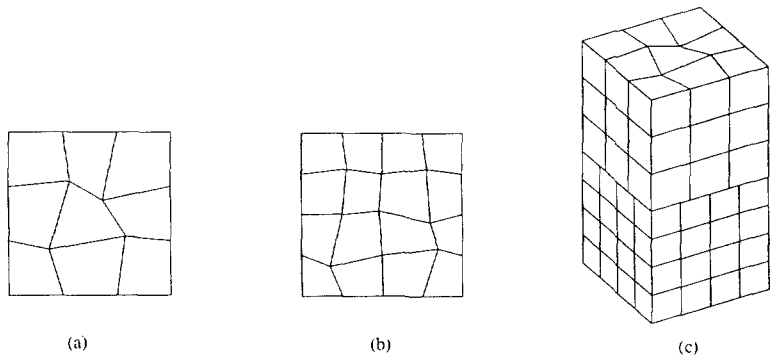

Figure 7: (a) Mesh pattern on upper surface. (b) Mesh pattern on bottom surface. (c) Upper and lower meshes at contact interface and subjected to homogenous stress (σ_z).

2. The outer sphere is then rotated (Figure 5) through 45 deg in 20 steps (2.25 deg per step).

The applied moment was analytically calculated to be 4.93071×10^8. Simulations using four different meshes were made: 96 elements, 384 elements, 864 elements and 7776 elements[3]. The moments computed in simulations using both smoothed and non-smoothed contact for the four different meshes is shown in Figure 6. The non-smoothed cases using 96, 384 and 864 elements were orders of magnitude off and were not shown. The computed moment for the 7776 element mesh using smoothing was exact within four decimal places of the analytical solution. The 96 element mesh with smoothing produced very good results for small rotations and overall was nearly as good as the 7776 element non-smoothed mesh. As seen in Figure 1., the smoothed surface gives a good representation of a sphere with a relatively coarse mesh. A convergence tolerance of 1×10^{-16} and 1×10^{-5} was used with the smoothed and non-smoothed contact respectively. In many time steps using the non-smoothed method, convergence could not be achieved in 20 steps. Nevertheless, the analysis was forced to proceede to the next time step to facilitate a solution.

4.2 Example 2: patch test

In this example, the patch test is considered for both the node on facet and mortar methods and their smoothed and non-smoothed implementations. When elements are rectangular, the node on facet algorithms solve the patch test exactly as do the mortar methods of course. Figure 7. shows the mesh used for a warped facet patch test where two blocks (Figure 7.a,b) are contacting. Using the mortar integral integration approach given in [15], the non-smoothed and smoothed mortar methods are exact to 8 and 5 decimal places respectively. The error is due to the inaccuracies of integration. Integration schemes that exactly satisfy this patch test are available and will be presented in future work. Errors for the two pass node on facet technique are 0.31% and 1.65% for non-smoothed and smoothed contact respectively. These errors are not exorbitant but two pass algorithms are inherently unstable. The single pass errors ran about 6.0%-18.4% depending on which side the slave side was defined on and whether smoothing was used.

[3]Only the flexible elements are counted here, none of the rigid sphere elements are counted

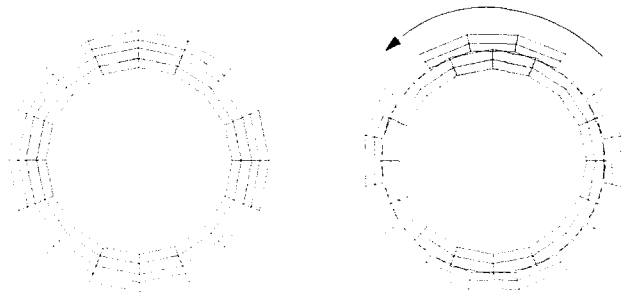

(a) (b)

Figure 8: (a) Concentric cylinders. (b) Concentric cylinders rotated.

Table 1: Maximum pressure for rotating cylinder

contact method	max. pressure
non-smooth node on segment	5.6×10^{-2}
smooth node on segment	1.5×10^{-3}
non-smooth mortar	5.1×10^{-4}
smooth mortar	1.9×10^{-5}

4.3 Example 3: rotating cylinders using node on facet and mortar methods

In this example, interference fits are evaluated for both node on facet and mortar methods, with and without smoothing. Since friction has not been implemented yet, a simpler test compared to Example 1 is used to evaluate the mortar methods. In this test, concentric cylinders (Figure 8) are rotated relative to each other and the internal pressure is checked to determine the amount of error in the interference fit. Identical materials are used for both cylinders and the outer cylinder cannot expand radially along the outer boundary whereas the inner boundary of the inner cylinder is free. Ideally, the internal pressure should be zero. The results for the different cases are shown in Table 1. The smoothed node on segment (2D) method is 36 times better than the non-smoothed method. Surprisingly, the non-smooth method is about 3 times better than the smoothed node on segment. Finally the smoothed mortar method is 27 times better than the non-smoothed method. Overall, the smooth mortar method is about 3000 times better than the classic non-smooth node on segment. This represents a significant improvement in the technology.

5 Discussion

In this work, smoothed node on facet and mortar contact algorithms were presented. It was found that smoothing can vastly improve convergence behavior for node on facet algorithms. Furthermore, better surface representation can be acquired by smoothing for both node on facet and mortar methods. Further investigation of smooth mortar element methods is in process.

References

[1] J. Hallquist, G. Goudreau, D. Benson, *Sliding interfaces with contact-impact in large-scale lagrangian computations*, Computer Methods in Applied Mechanics and Engineering, 51, (1985), 107–137.

[2] M. Puso, T. Laursen, *A 3d contact smoothing algorithm using gregory patches*, International Journal for Numerical Methods in Engineering, to appear.

[3] P. Papadopoulos, R. Taylor, *A mixed formulation for the finite element solution of contact problems*, Computer Methods in Applied Mechanics and Engineering, 50, (1992), 163–180.

[4] J. Simo, P. Wriggers, R. Taylor, *A perturbed lagrangian formulation for the finite element solution of contact problems*, Computer Methods in Applied Mechanics and Engineering, 50, (1985), 163–180.

[5] P. Hild, *Numerical implementation of two nonconforming finite element methods for unilateral contact*, Computer Methods in Applied Mechanics and Engineering, 184, (2000), 99–123.

[6] B. Wohlmuth, *A mortar finite element method using dual spaces for the lagrange multiplier*, Society for Industrial and Applied Mathematics, 38, (2000), 989–1012.

[7] F. Belgacem, P. Hild, P. Laborde, *The mortar finite element method for contact problems*, Mathematical and Computer Modeling, 28, (1998), 263–271.

[8] F. Belgacem, P. Hild, P. Laborde, *Approximation of the unilateral contact problem by the mortar finite element method*, Comptes Rendus De L'Academie Des Sciences, 324, (1997), 123–127.

[9] K. Park, C. Felippa, *A simple algorithm for localized construction of non-matching structural interfaces*, International Journal for Numerical Methods in Engineering, 53, (2002), 2117–2142.

[10] G. Farin, *Curves and Surfaces for Computer-Aided Geometric Design*, Academic Press, London, fourth edn. (1997).

[11] J. Foley, et al., *Computer Graphics, Principles and Practice*, Addison-Wesley, Reading, second edn. (1997).

[12] H. Chiyokura, F. Kimura, *Design of solids with free form surfaces*, Computer Graphics, 17, (1983), 289–298.

[13] B. Wohlmuth, *Discretization Methods and Iterative Solvers Based on Domain Decomposition*, Springer-Verlag, Heidelberg (2001).

[14] M. Puso, T. Laursen, *A 3d mortar method for solid mechanics*, International Journal for Numerical Methods in Engineering, to be submitted.

[15] M. Puso, T. Laursen, *Mesh tying on curved interfaces in 3d*, Engineering Computations, submitted.